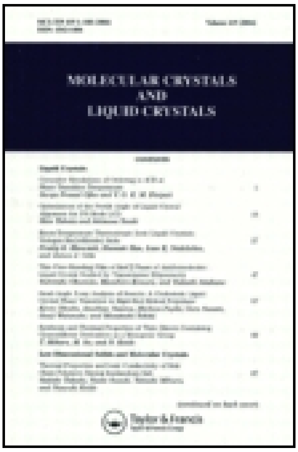

Molecular Crystals and Liquid Crystals
Publication details, including instructions for authors and subscription information:
http://www.tandfonline.com/loi/gmcl20

Elementary Excitations in Quantum Antiferromagnetic Chains: Dyons, Spinons and Breathers

T. Asano [a] , H. Nojiri [b] , Y. Inagaki [a] , Y. Ajiro [a] , L. P. Regnault [c] & J. P. Boucher [d]

[a] Department of Physics, Kyushu University, Fukuoka, 812-8581, Japan

[b] Department of Physics, Okayama University, Okayama, 700-8530, Japan

[c] Laboratoire de Magnétisme et de Diffraction Neutronique, CEA, DRFMC-SPSMS, Grenoble, 38054, France

[d] Laboratoire de Spectrométrie Physique, Université J. Fourier-Grenoble 1, Saint-Martin d'Hères, 38402, France

Version of record first published: 18 Oct 2010

Mol. Cryst. Liq. Cryst., Vol. 379, pp. 121-130
Copyright © 2002 Taylor & Francis
1058-725X/02 $12.00 + .00
DOI: 10.1080/10587250290090363

Elementary Excitations in Quantum Antiferromagnetic Chains: Dyons, Spinons and Breathers

T. ASANO[a], H. NOJIRI[b], Y. INAGAKI[a], Y. AJIRO[a], L. P. REGNAULT[c] and J. P. BOUCHER[d]

[a]*Department of Physics, Kyushu University, Fukuoka 812-8581, Japan,*
[b]*Department of Physics, Okayama University, Okayama 700-8530, Japan,*
[c]*DRFMC-SPSMS, Laboratoire de Magnétisme et de Diffraction Neutronique, CEA, 38054 Grenoble, France and*
[d]*Laboratoire de Spectrométrie Physique, Université J. Fourier-Grenoble 1, 38402 Saint-Martin d'Hères, France*

Considering experimental results obtained on three prototype compounds, TMMC, $CsCoCl_3$ (or $CsCoBr_3$), and Cu Benzoate, we discuss the importance of non-linear excitations in the physics of quantum (and classical) antiferromagnetic spin chains.

Keywords: soliton; dyons; spinons; breathers.

INTRODUCTION

In the last twenty years, various experimental and theoretical studies have been devoted to antiferromagnetic chains (AFC). One fascinating problem concerns the nature of the elementary excitations in such systems. As a crucial ingredient one has to refer to the concept of non-linear excitations (NLE). Typical examples of NLE are provided by the *solitons* and the *breathers*. These particular excitations are solutions of the so-called *sine-Gordon* equation[1]. The first evidence of solitons in AF chains was obtained on a classi-cal spin system (in the 80's)[2]. Recently, evidence for breathers was obtai-ned on a quantum spin system[3]. A short review is presented, where the role of the NLE in AFC is discussed. The case of anisotropic spin models is consi-dered explicitly and a relation with the isotropic case is proposed. Quantiza-tion effects are also shown to play a crucial role: for the solitons, this leads to the concept of *dyons*; for the breathers to a discretization of the excitation spectrum. Along this paper, we shall refer explicitly to three compounds: $(CH_3)_4NMnCl_3$, alias TMMC, two Co compounds, $CsCoCl_3$ and $CsCoBr_3$[4],

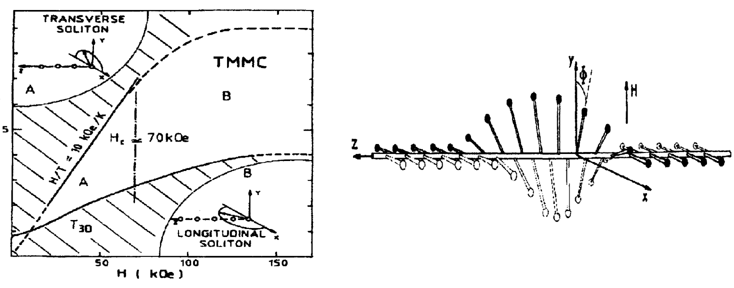

a b

FIGURE 1 a) Soliton phase diagram of TMMC[4]. H_c is the cross-over field between the soliton regimes A and B (see the insets). b) Schematic representation of a soliton in TMMC.

and $Cu(C_6H_5COO)_2.3H_2O$, alias Cu Benzoate[3]. All of them are known to provide examples of 1-dimensional AFC. In TMMC, the spin value is large, s=5/2, and a semi-classical spin description can be used. The other compounds are representative of quantum spin systems, with s=1/2.

TMMC

TMMC is an example of quasi-isotropic Heisenberg AFC. At T_{co}~20 K, because of the small dipolar anisotropy D, a crossover occurs, which changes the spin system from isotropic to easy-plane behaviors[5]. The spins can be viewed as being repelled in the XY plane perpendicular to the chain Z direction. Then, if one applies a magnetic field H in the XY plane - along the Y axis, for instance - another crossover occurs: the spins become mainly aligned along the X axis, in the spin-flop configuration. They form an Ising-like AF spin system where the soliton regime takes place. The soliton phase diagram for TMMC is shown in Figure 1a[4]. Two soliton regimes (A and B in Figure 1a, see also the insets) can be defined, which both correspond to the sine-Gordon model. In regime A, the effective anisotropy is due to D, in regime B, it is induced by H[4]. We mainly limit the discussion to the “transverse” soliton regime A. For TMMC, the initial Hamiltonian is given by:

$$\aleph = \Sigma\ 2J\ \mathbf{s}_n\mathbf{s}_{n+1} - 2D\ s^z{}_n s^z{}_{n+1} - g\mu_B H s^y{}_n \quad (1)$$

with J ~ 6.8 K and D ~ 0.16 K and s =5/2. Each spin can be described as a vector, the orientation of which is defined by two angles, θ and ϕ. In configuration A, the spins are assumed to remain within the XY plane. Accordingly, $\theta \sim \pi/2$, and ϕ is defined by the angle between the spin and H. In the Ising-like phase of TMMC, the spin vectors can simply be written $s^y_n = (-1)^n \cos\phi$. A classical description - in the continuum limit and after the variable change $\psi = \pi - 2\phi$ - transforms (1) into

$$\aleph = Js^2/2 \int_{-\infty}^{+\infty} dz\{1/2[1/C^2(\partial\psi/\partial t)^2 + (\partial\psi/\partial z)^2 + m^2(1-\cos(\psi)) \qquad (2)$$

which is the hamiltonian of the sine-Gordon model. Here, $C=4Js[1-D/(2J)]^{1/2}$ defines the soliton velocity and $m=g\mu_B H/4Js$ the soliton mass. The elementary excitations are NLE: the solitons (and antisolitons) and the breathers. A soliton in TMMC (or an antisoliton) is to be viewed as a domain wall (extending over several lattice spaces), with a well-defined shape as represented in Figure 1b. The breather modes are soliton-antisoliton boundstates. As a general property, when NLE move along the chains, they maintain an exact balance between two energy contributions, the "potential" and the "internal" energies defined by the two last terms of (2), respectively. This explains the remar-kable "integrity" of the NLE excitations[1].

A soliton is associated with a π rotation of the spins (see Figure 1b). From the study of the fluctuations, an accurate description of the soliton regimes in TMMC has been obtained[2,6]. In spin systems, a discretization of the breather spectrum is to be expected, giving rise to distinct excitation branches, hereafter denoted $B_l \ldots B_n$. In the A regime, the lowest B_l coincides with the usual magnon branch[7] associated with the energy gap $E_l^A = g\mu_B H$. Because to the two competitive anisotropies (D and that induced by H), there exists a second magnon branch associated with the gap: $E_l^B = 4S\sqrt{(DJ)}$ (~0.8 meV). This higher gap is that of the lowest breathers for the B soliton regime. The quantization process of the breathers applies simultaneously to the A and B regimes. Additional peaks are therefore expected at energies $E \sim E_l^B \pm E_l^A$, in agreement with the observation[8].

THE Co COMPOUNDS: $CsCoCl_3$ and $CsCoBr_3$

An alternative soliton (or kink) model for AF chains has been proposed by J. Villain in 1975[9]. It applies to the following quantum (s = ½) Ising-like Hamiltonian[10]:

$$\aleph = 2J \Sigma s^z_n s^z_{n+1} + \varepsilon (s^x_n s^x_{n+1} + s^y_n s^y_{n+1}) \qquad (3)$$

with $\varepsilon \ll 1$. The groundstate is the Néel state represented in Figure 2a. The first excited state is displayed in Figure 2b: it contains a (one-lattice) domain wall. The corresponding soliton excitation branch is displayed in Figure 3Aa. The arrows show the transitions to be realized in experiments. The transitions shown by the dash arrow (i.e., induced from the groundstate) are forbidden.

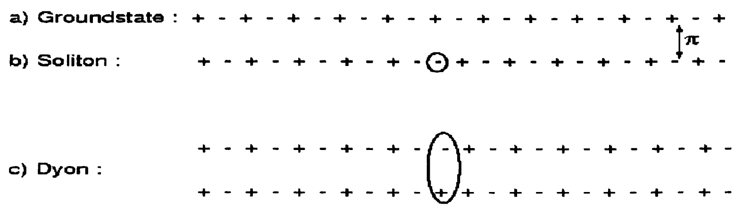

FIGURE 2 a) Dispersions of the soliton excitations in the Villain model: the solid line is for a small ε value; the dashed line, for a large ε (→1). The arrows illustrate experimental transitions (see text). b) the fluctuation spectrum of the (individual) soliton mode (in zero field).

They would require that an infinite number of spins be simultaneously flipped (to achieve the π rotation of the sublattices). Only transitions inside the soliton branch (shown by the full arrow) are allowed: they describe the fluctuations of (individual) solitons. The corresponding spectrum is drawn in Figure 3Ab: it is characterized by a single peak at $E_{max}(q) = 4\varepsilon J \sin(q)$[6,11].

As shown in Figure 2c, such a soliton is, in fact, a doublet, which is defined by the quantum spin number S = ½. In a field H, one expects a Zeeman splitting as shown in Figures 3Ba and 3Bb, for H parallel ($H_{//}$) and perpendicular ($H_{\perp}$) to the Z axis. The allowed transitions take place now

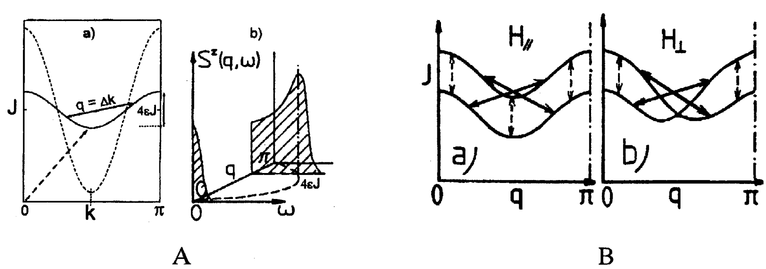

FIGURE 3 A: a) Dispersions of the soliton excitations in the Villain model: the solid line is for a small ε value; the dashed line, for a large ε (→1). The arrows illustrate experimental transitions (see text). b) The fluctuation spectrum of the (individual) soliton mode (in zero field). B: Zeeman splitting of the soliton dispersion in the Villain model for a field parallel (a) and transverse (b) to the Ising direction.

between the two split branches (the full arrows in Figures 3B). Finally, this effect results in a "*doubling*" of the individual soliton modes (Figures 4Aa and 4Bb)[12].

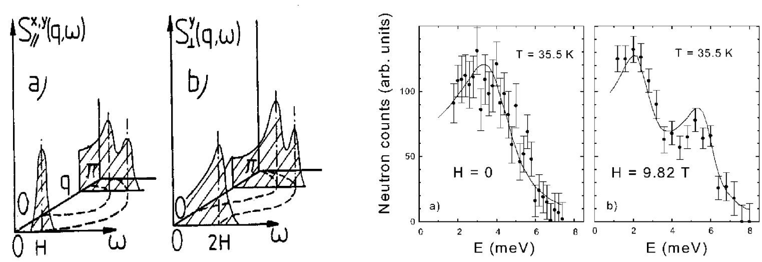

A B

FIGURE 4 A: Doubling of the soliton modes in the Villain model, for H parallel (a) and perpendicular (b) to the Ising direction. B: NIS on $CsCoBr_3$: a) Soliton mode in zero field; b) Doubling of the soliton mode in a transverse field. These energy scans correspond to the wavevector transfer q $= \pi/2$.

$CsCoCl_3$ and $CsCoBr_3$ are good examples of the Villain model, with J~75 K and ε~0.12. The fluctuations of the (individual) soliton modes have been observed by neutron inelastic scattering (NIS) on $CsCoBr_3$[13]. In these first measurements, however, the presence of a "peak" was not convincingly established. Measurements with a higher instrumental resolution have been performed at the Institut Laue-Langevin (ILL, Grenoble, France) using the IN14 spectrometer[14]. An example of the soliton mode in zero field, for the wavevector transfer $\Delta k = q = \pi/2$, is shown in Figure 4Ba. The presence of a peak, or at least a maximum, is now established. Its position agrees well with the theory (the full line, which takes into account the instrumental resolution, δE~1 meV). In Figure 4Bb, the same energy scan performed in presence of a magnetic field ($H_\perp = 9.82$ T) is reported. Two maxima are now visible: this is in complete agreement (the full line is the theory) with the predicted doubling of the soliton modes.

Transitions for a $\Delta k = 0$ wavevector transfer - the vertical dashed arrows in Figure 5 - are realized in an ESR experiment. Such ESR, referred to as Soliton Magnetic Resonance (SMR), have been performed on $CsCoCl_3$[15]. A few examples of SMR signals are reported in Figure 5, for both $H_{//}$ and $H_\perp$. The agreement with the theory (the full lines) is also very good. From these NIS and SMR measurements, the S = ½ quantum nature of the soliton state in the Co compounds is well established.

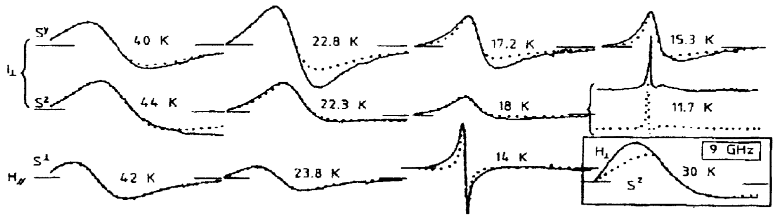

FIGURE 5 SMR signals observed in $CsCoCl_3$, for H parallel and H perpendicular to the Ising direction.

This result is rather general: it applies to systems with large spin values (s > ½) as well. As shown by Haldane[16], a soliton in AFC contains internal degrees of freedom. A quantization results in a discretization of the soliton states, with, however, a crucial difference between integer and half-integer spin chains: in the former case, the lowest soliton state is a S=0 excitation (this is the basis of the "Haldane conjecture"), while in the later case, it is a S=½ excitation (in agreement with the results on the Co compounds). We may also refer to the *dyon* concept introduced by Affleck: the S=½ solitons as observed in the Co compounds are dyon analogs in quantum AFC[17].

QUANTUM ISOTROPIC SPIN CHAINS

Up to now, we have considered anisotropic systems where the NLE are rigorously defined. To reach a similar physical picture for isotropic chains, we apply the discussion presented by Haldane for classical spin systems[16] to the quantum Villain model. When $\varepsilon \rightarrow 1$ in (3), the amplitude of the dispersion increases as shown by the dashed line in Figure 3Aa. At $\varepsilon = 1$, i.e., for the isotropic Heisenberg hamiltonian

$$\aleph = \Sigma\, 2J\, \mathbf{s}_n \mathbf{s}_{n+1} \tag{4}$$

the gap of the soliton branch closes at $k = \pi/2$. A phase transition occurs[18], which can be viewed as an isolant-metal transition[19]. The dyon states (i.e., the pairs of + ½ and – ½ solitons) are seen to fill in the groundstate of the isotropic phase. In this limit, one is used to refer to a different concept, the *spinon* concept[20]. A spinon is defined as an "entity" associated with a ± ½ spin value and the groundstate is made of *pairs* of spinons.

The description of quantum Heisenberg chains starts with the Bethe ansatz (1931)[21]. In the 60's, based on the Jordan-Wigner (JW) transformation, it was used to refer to a model of strongly-interacting fermions[22]. In the 70's, more sophisticated analyses were proposed [23], which yields the modern field-theoretic derivations, which in the recent years, have renewed and enlarged our understandings of so many quantum spin systems. Cu Ben-zoate is a recent example: the derivation leads to a sine-Gordon model[24].

In isotropic systems, there is no definite direction for the spins [i.e., no angle ψ as in (2)]. The JW transformation is used first and a fermionic representation of the hamiltonian is obtained [with, in reciprocal space, the fermions operators α_q (α^+_q) and β_q (β^+)]. In the low energy limit, the significant physical quantities turn out to be related, not to the fermions, but to the fermion densities: $\rho^+_q \sim \Sigma_k\, \alpha^+_{k+q}\, \alpha_k$ and $\rho^-_q \sim \Sigma_k\, \beta^+_{k+q}\, \beta_k$ (this is the "bozonization"). Finally, back to real space, a new field "$\psi°$" can be defined, and, hamiltonian (4) becomes

$$\aleph = J/8 \int^{+\infty}_{-\infty} dz\{1/2[(\partial\psi°/\partial z)^2 + 1/C^{o2}(\partial\psi°/\partial t)^2\} \qquad (5)$$

with $C°=\pi$ J. In this expression, the field $\psi°$ does not compare to the angle ψ introduced in (2): $\psi°$ is now related to the fermion densities ρ^+_q and ρ^-_q. Eq. 5 is not the sine-Gordon Hamiltonian. The non-linearity [the last term in (5)] is missing. Accordingly, the excitations of (5) follow *linear* dispersions (i.e., *no energy gap*). They describe the lowest part of the *spinon continuum* characterizing the excitation spectrum of (4). The application of a field H on hamiltonian (4) develops a "dynamical incommensurability": the wavevectors where the zero-energy fluctuations develop are shifted by $\delta q_{inc} = 2\pi\, \sigma$, where σ is

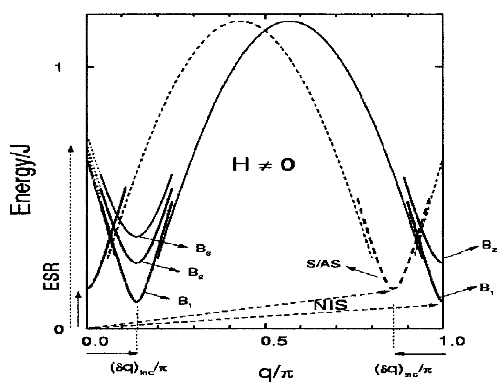

FIGURE 6 A model for the dispersion of the elementary excitations in Cu Benzoate: the soliton/antisoliton branch gives a gap at q = 0 and at the incommensurate wavevector q = π - δq_{inc}. The breather branches give a gap at q = π and at the incommensurate wavevector q = δq_{inc}. The dashed arrows corresponds to NIS[26], the full arrows to ESR[3].

the magnetization per spin (an increasing function of H). The dispersions, however, remain linear at low energy and *no energy gap* is induced by a field.

Cu BENZOATE

In the 70's, CuBenz was considered as a good example of quantum isotropic AFC[25]. Recently, however, it has been observed that, in a field, an energy gap opens[26], in contradiction with the above discussion. As established by Affleck and Oshikawa[24], this behavior is due to the presence an additional "staggered" field, h_{st}[27] and the effective hamiltonian is

$$\aleph = \Sigma_n 2J\, \mathbf{s}_n \mathbf{s}_{n+1} - g\mu_B H s^z_n - g\mu_B\, h_{st}\, (-1)^n\, s^x_n \qquad (6)$$

with J~5.8 K, and where h_{st} is proportional to the applied field: h_{st}~0.09H (for H applied parallel to the c axis)[28]. The field-theoretic derivation of this hamiltonian[24] transforms (6) into the sine-Gordon equation:

$$\aleph = J/8 \int^{+\infty}_{-\infty} dz\{1/2[(\partial\psi^\circ/\partial z)^2 + 1/C^{\circ 2}(\partial\psi^\circ/\partial t)^2 + m^2(1 - \cos(\psi^\circ)) \qquad (7)$$

where C° and the field ψ° are defined in a similar way as in (5). The soliton mass is now a function of the staggered field: $m \sim 1.85(h_{st}/J)^{2/3}\,|\log(h_{st}/J)|$ [24]. The low-energy excitations of (7) are solitons (antisolitons) and breathers. In Figure 6, a representation of the spectrum for Cu Benzoate is proposed. The bold lines correspond to the sine-Gordon predictions (low-energy limit). In this figure, only three breather branches are represented: B_1, B_2 and B_3.

In Figure 6, the transitions induced by NIS are represented by the dash arrows (these measurements were performed at one field value, H ~ 7 T)[26]. A dynamical incommensurability is observed at $q = \pi - \delta q_{inc}$ where the gap of the soliton/antisoliton branch is directly measured. At $q = \pi$, the two first breather modes, B_1 and B_2, are also detected[29]. The transitions observed by ESR[3] are shown by the vertical arrows (dot and solid): the soliton (anti-soliton) gap and the breathers are observed at q = 0 [30]. The field depen-dence (up to H~20 T) of the soliton gap measured by ESR is displayed in Figure 7A. In low field, the agreement with the sine-Gordon model (the full line) is rather good: E_G=mJ~$H^{2/3}$. An appreciable deviation, however occurs in high fields. Figure 7B shows the H dependence of the three first breathers, B_1, B_2 and B_3 probed by ESR.

CONCLUSION

With these three compounds - TMMC, the Co compounds and Cu Benzoate - the NLE are seen to play a crucial role both in classical and quantum AFC.

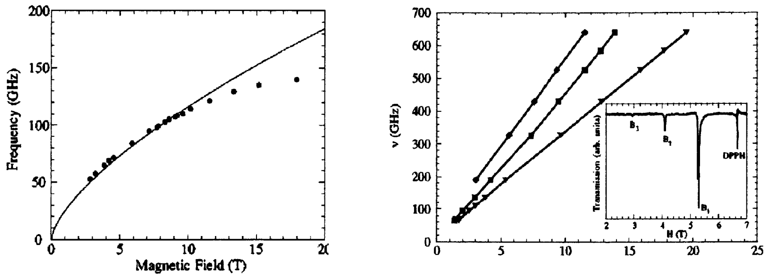

A B

FIGURE 7 A: Field dependence of the soliton gap observed by ESR (Voigt configuration) in Cu Benzoate. B: Field dependence of the first breather modes observed by ESR (Faraday configuration) in Cu Benzoate[3].

TMMC and Cu Benzoate are well described by the sine-Gordon model. Fundamental differences, however, occurs between the two systems. In the Ising-like chains (TMMC and the Co compounds), transitions from the groundstate to the soliton state are forbidden (the dash line in Figure 3Aa). The solitons are detected via their fluctuations[6,13]. In Cu Benzoate, however, the transitions from the groundstate to both the soliton and the breather branches are allowed (see the arrows in Figure 6Aa). With Cu Benzoate, the discretization of the breathers in a sine-Gordon system is well established.

Acknowledgements
One of us (JPB) would like to thank T. Ziman for useful discussions.

References
[1.] A. C. Scott, F.Y.F. Chu, and D. W. McLaughlin, *Proceedings of the IEEE*, **61**, 1443, (1973).
[2.] J.P. Boucher, L.P. Regnault, J. Rossad-Mignod, J.P. Renard, J. Bouillot and W.G. Stirling, *Sol. Stat. Comm.*, **33**, 171 (1980).
[3.] T. Asano, H. Nojiri, Y. Inagaki, J.P. Boucher, T. Sakon, Y. Ajiro, and M. Motokawa, *Phys. Rev. Lett.*, **84**, 5880 (2000).
[4.] For a review on solitons in TMMC and the Co compounds, see for instance: J.P. Boucher, L.P. Regnault, and H. Benner, in Nonlinearity in Condensed Matter, Springer Series in Solid State-Sciences, Vol. **69**, 24 (1987).
[5.] J.P. Boucher, L.P. Regnault, J. Rossad-Mignod and J. Villain, *J. M. M. M.*, **14**, 155, (1979).
[6.] In TMMC, both the fluctuations associated with the flipping process of the sublattices, and those associated with the individual solitons have been

observed: J.P. Boucher, L.P. Regnault, R. Pynn, J. Bouillot, and J.P. Renard, *Europhys. Lett.*, **1**, 415 (1986).
[7.] K. Maki and H. Takayama, *Phys. Rev.*, **B22**, 5302 (1980).
[8.] J.P. Boucher, R. Pynn, M. Remoissenet, L.P. Regnault, Y. Endoh, and J.P. Renard, *Phys. Rev. Lett.*, **64**, 1557 (1990).
[9.] J. Villain, *Physica B* **79,** 1 (1975).
[10.] For the Villain model, several derivations have been proposed. In a second quantization approach, the solitons have been shown to be fermions: F. Devreux and J.P. Boucher, *J. Phys.*, (France) **48**, 1663 (1987).
[11.] A limitation of the diverging peak results from the collisions between solitons: K. Sasaki and K. Maki, *Phys. Rev.,* **B35**, 257 (1987).
[12.] J.P. Boucher, in Magnetic Excitations and Fluctuations II, Proceedings in Physics **23**, p. 171, (1987), edited by: U. Bucalani, S. W. Lovesey, M.G. Rasetti and V. Tognetti, Springer Verlag.
[13.] H. Yoshizawa, K. Hirakawa, S.K. Satija, and G. Shirane, *Phys. Rev.*, **B23**, 2298 (1981); S.E. Nagler, W.J.L. Buyers, R.L. Armstrong, and B. Briat, *Phys. Rev. Lett.*, **49**, 590 (1982); J.P. Boucher, L.P. Regnault, J. Rossad-Mignod, J.Y. Henry, J. Bouillot and W.G. Stirling, *Phys. Rev.*, **B31**, 3015 (1985).
[14.] J.P. Boucher, L.P. Regnault, R; Currat, J.Y. Henry, ILL Report 1990.
[15.] J.P. Boucher, G. Rius, and J.Y. Henry, *Europhys. Lett.*, **4**, 1073 (1987).
[16.] F.D.M. Haldane, *Phys. Rev. Lett.*, **50**, 1153 (1983).
[17.] I. Affleck, *Phys. Rev. Lett.*, **57**, 1048 (1986).
[18.] R.R.P. Singh, *Phys. Rev.*, **B5,** 11582 (1996).
[19.] H. J. Schulz, in Proceedings of Les Houches Summer School LXI, ed. E. Akkermans, G. Montambaux, J. Pichard, et J. Zinn-Justin (Elsevier, Amsterdam, 1995), p.533.
[20.] L.D. Fadeev and L.A. Takhtajan, *Phys. Lett.*, **85A**, 375 (1981).
[21.] H. Bethe, *Z Physik*, **71**, 205 (1931).
[22.] For instance, L.N. Bulaevskii, *Sov. Phys. JETP*, **16**, 685 (1963).
[23.] For instance, A. Luther and I. Peschel, *Phys. Rev.*, **B12**, 3908 (1975); J. Solyom, in Lectures notes in Physics 96, Quasi one-Dimensional II, p. 20, 1978; Springer-Verlag.
[24.] I. Affleck and M. Oshikawa, *Phys. Rev.*, **B60**, 1038 (1999).
[25.] K. Okuda, H. Hata, and M. Date, *J. Phys. Soc. Jpn.*, **33**, 1574 (1972).
[26.] D.C. Dender, P.R. Hammar, D.H. Reich, C. Broholm and G. Aeppli, *Phys. Rev. Lett.*, **79**, 1750 (1997).
[27.] This staggered field results from two contributions: one is due to the g factor, which undergoes a small alternation along the chain, the other to the presence of small Dzyaloshinski-Moryia interactions (see [24]).
[28.] M. Oshikawa and I. Affleck, *Phys. Rev. Lett.*, **79**, 2883 (1997).
[29.] F.H.L. Essler and A.M. Tsvelik, *Phys. Rev.*, **B57**, 10592 (1998).
[30.] M. Oshikawa and I. Affleck, *Phys. Rev. Lett.*, **82**, 5136 (1999).